Psychiatry Research: Neuroimaging 273 (2018) 54–62

Contents lists available at ScienceDirect

Psychiatry Research: Neuroimaging

journal homepage: www.elsevier.com/locate/psychresns

Preliminary mapping of the structural effects of age in pediatric bipolar disorder with multimodal MR imaging

Ryan P. Cabeen[a,*], David H. Laidlaw[b], Amanda Ruggieri[c], Daniel P. Dickstein[c]

[a] Laboratory of Neuro Imaging, USC Stevens Neuroimaging and Informatics Institute, Keck School of Medicine of USC, University of Southern California, Los Angeles, CA, USA

[b] Department of Computer Science, Brown University, Providence, RI, USA

[c] Pediatric Mood, Imaging & NeuroDevelopment Program, Bradley Hospital, Alpert Medical School of Brown University, Providence, RI, USA

ARTICLE INFO

Keywords:
Pediatric bipolar
Adolescents
Magnetic resonance imaging
Diffusion tensor imaging
Cortical thickness
Tractography

ABSTRACT

This study investigates multimodal structural MR imaging biomarkers of development trajectories in pediatric bipolar disorder. T1-weighted and diffusion-weighted MR imaging was conducted to investigate cross-sectional group differences with age between typically developing controls (N = 26) and youths diagnosed with bipolar disorder (N = 26). Region-based analysis was used to examine cortical thickness of gray matter and diffusion tensor parameters in superficial white matter, and tractography-based analysis was used to examine deep white matter fiber bundles. Patients and controls showed significantly different maturation trajectories across brain areas; however, the magnitude of differences varied by region. The rate of cortical thinning with age was greater in patients than controls in the left frontal pole. While controls showed increasing fractional anisotropy (FA) and axial diffusivity (AD) with age, patients showed an opposite trend of decreasing FA and AD with age in fronto-temporal-striatal regions located in both superficial and deep white matter. The findings support fronto-temporal-striatal alterations in the developmental trajectories of youths diagnosed with bipolar disorder, and further, show the value of multimodal computational techniques in the assessment of neuropsychiatric disorders. These preliminary results warrant further investigation into longitudinal changes and the effects of treatment in the brain areas identified in this study.

1. Introduction

Research during the past two decades has demonstrated that bipolar disorder (BD) is an escalating problem among children and adolescents. While once thought to be rare, studies have demonstrated that 20–40% of adults diagnosed with BD report that their illness started during childhood or adolescence, rather than adulthood (Leboyer et al., 2005; Baldessarini et al., 2010, 2012). Moreover, several studies have shown increasing numbers of children and adolescents are being diagnosed with BD. For example, the percentage of children and adolescents discharged from United States (U.S.) psychiatric hospitals with a diagnosis of BD has increased, from less than 10% in the mid-1990s to more than 20% in the mid-2000s (Blader and Carlson, 2007). This is not only an inpatient phenomenon, as Moreno et al. found a forty-fold rise in the incidence of outpatient visits made to providers of all specialties for a diagnosis of BD during a similar period, from 25/100,000 in 1993–1994 to 1003/100,000 in 2002–2003 (Moreno et al., 2007). Furthermore, this is not just a diagnostic trend confined to the U.S., as rates of German children under age 19 years old admitted to psychiatric hospitals for BD surged 68.5%—from 1.13/100,000 in 2000 to 1.91/100,000 in 2007, an increase greater than the general trend for mental health disorder admissions (Holtmann et al., 2010). To address the problem of rising numbers of children and adolescents being diagnosed with BD, we need greater understanding of the underlying neural mechanisms which could ultimately improve the specificity of our diagnostic and treatment approaches to pediatric BD. Mechanisms matter, as has been shown from other areas of biomedical research. For example, greater understanding of the mechanisms of childhood leukemia has resulted in better, more specific diagnostic approaches whereby suspicion of clinical symptoms (e.g., easy bruising, weakness, swollen abdomen) is confirmed (or ruled out) by a biomarker (e.g., a complete blood count). A similar approach using biological and behavioral mechanisms to augment clinical diagnosis could improve the specificity of how children are diagnosed as having BD (or not).

Towards that end, structural and functional magnetic resonance imaging (MRI) has been used as a tool to investigate such neural mechanisms, and previous studies have implicated the fronto-temporal-striatal circuit in pediatric BD. Specifically, structural MRI studies have

* Corresponding author.
E-mail address: rcabeen@ini.usc.edu (R.P. Cabeen).

https://doi.org/10.1016/j.pscychresns.2017.12.006
Received 30 May 2017; Received in revised form 31 December 2017; Accepted 31 December 2017
Available online 10 January 2018
0925-4927/

found significantly decreased gray matter volume of the amygdala vs. typically-developing controls (TDC) (Blumberg et al., 2003; DelBello et al., 2004; Chang et al., 2005; Dickstein et al., 2005; Pfeifer et al., 2008; Hajek et al., 2009), as well as some studies showing similar decreases in the left dorsolateral prefrontal cortex (DLPFC) (Dickstein et al., 2005). Functional MRI (fMRI) studies have shown fronto-temporal-striatal alterations in tasks tapping functions including face processing (Dickstein et al., 2007; Pavuluri et al., 2007; Rich et al., 2008; Brotman et al., 2009; Kalmar et al., 2009; Kim et al., 2012; Wiggins et al., 2017), response inhibition (Leibenluft et al., 2007a, 2007b; Singh et al., 2010a, 2010b), response to frustration (Deveney et al., 2013; Rich et al., 2010), cognitive flexibility (Dickstein et al., 2010; Adleman et al., 2011), and resting state connectivity (Stoddard et al., 2015).

Diffusion-weighted MRI (dMRI) is a complementary structural neuroimaging modality used to characterize brain white matter by probing patterns of water molecule motion in tissue. Imaging metrics derived from dMRI datasets provide a unique probe for detecting changes in myelination, fiber organization, and axonal morphometry (Basser and Pierpaoli, 1996; Beaulieu, 2002), and previous dMRI studies have used them to reveal disruptions in tissue microstructure and connectivity that are related to BD. Of the approximately 16 currently published original data dMRI studies of BD youths, all have examined tensor-derived imaging metrics and shown decreased, rather than increased, fractional anisotropy (FA)—a scalar value of the degree of anisotropy of the diffusion process, with zero indicating isotropic diffusion, and one indicating anisotropic/restricted diffusion—and disrupted white matter integrity. This includes decreased FA among BD vs. TDC youths in the anterior corona radiata (Adler et al., 2006; Pavuluri et al., 2009; Lagopoulos et al., 2013), the corpus callosum (Ishida et al., 2017; James et al., 2011; Saxena et al., 2012; Lagopoulos et al., 2013), white matter adjacent to cingulate cortex (Frazier et al., 2007; Gao et al., 2013; Gönenç et al., 2010), white matter areas adjacent to prefrontal cortex (PFC) and orbitofrontal cortex (Adler et al., 2004; Kafantaris et al., 2009). BD youths also have decreased FA in deep white matter regions, including the fornix (Barnea-Goraly et al., 2010) and internal capsule (Lu et al., 2012). Predictive modeling has also shown promising results. For example, in the recent study by Mwangi et al. that trained a support vector machine (SVM) algorithm to predict the diagnostic status of youths with BD ($N = 16$) vs. TDC ($N = 16$) youths with 87.5% specificity, 68.75% sensitivity, 78.12% accuracy, and 84.62% positive predictive value (Mwangi et al., 2014). Taken in whole, these studies suggest that decreased FA and disrupted white matter integrity may be involved in the pathophysiology of pediatric BD.

Moving the field forward requires that studies integrate these different MRI modalities, as it can help to more comprehensively evaluate the effect of development on BD vs. TDC alterations across different structures and tissue types. With respect to integrating T_1-weighted and diffusion-weighted MRI, James et al. found decreased gray matter density by voxel based morphometry (VBM) in the left orbitofrontal cortex and decreased FA in the anterior cingulate cortex by tract based spatial statistics (TBSS) among BD ($N = 15$) vs. TDC ($N = 20$) youths (James et al., 2011). With respect to potential developmental effects, Toteja et al. found lower FA and higher mean diffusivity (MD; the average total diffusion within a voxel) among BD vs. controls (14 youths and 43 adults in each group), and significantly greater MD among BD participants at all ages than controls (whereas this was not significant for FA) (Toteja et al., 2015).

In the present study, we sought to conduct a preliminary analysis to extend the scope of such integrated studies by performing a more comprehensive analysis of both structural T_1-weighted MRI and dMRI among BD and TDC youths ages 8–17 years old. Based on prior studies, we hypothesized that BD youths would have decreased fronto-temporal-striatal thickness and decreased white matter connectivity among these regions, and that the change of imaging metrics across age is a potentially useful biomarker. To test these hypotheses, we employed novel computational image analyses to characterize regional variation in both cortical thickness and diffusion MR metrics reflecting variation in white matter microstructure and connectivity. Unlike other prior studies, such as those using tract-based spatial statistics (TBSS), the present study unites both structural MRI via cortical thickness with dMRI via multi-compartment tractography modeling (Behrens et al., 2007), which can help resolve complex sub-voxel fiber configurations in white matter and improve the anatomical accuracy and reliability of bundle reconstructions (Cabeen et al., 2016).

2. Methods

2.1. Participants

Participants included children and adolescents ages 8–17 years old who were enrolled in an Institutional Review Board approved research study. Written informed parental consent and child assent were obtained prior to participation. The rationale for this age range was to span the breadth of childhood and adolescence to examine neural alterations associated with BD vs. typical development (as supported by K22MH074945 awarded to DPD).

For all participants, psychopathology was assessed using the Kiddie Schedule for Affective Disorders and Schizophrenia, Present and Lifetime Version (K-SADS-PL) administered to parents and children separately by either a board-certified child/adolescent psychiatrist (DPD) or a licensed clinical psychologist (KLK, κappa > 0.85 for diagnoses). Comorbidity within the BD group was assessed by asking about symptoms and impairments during periods of generally euthymic mood to avoid counting manic or depressive symptoms more than once.

Inclusion criteria for all participants were: (1) age between 8 and 17 years, (2) English fluency, and (3) a consenting parent/guardian. Exclusion criteria were: Wechsler Abbreviated Scales of Intelligence Full Scale IQ (WASI FSIQ) ≤ 70; substance/alcohol abuse or dependence within the last 2 months; primary psychosis or autism spectrum disorders; and medical/neurological conditions that mimic BD.

BD group ($N = 26$) inclusion criteria were meeting DSM-IV-TR criteria for BD, including a history of at least one hypomanic (≥ 4 days) or manic (≥ 7 days) episode in which the child exhibited abnormally elevated or expansive mood, and three or more DSM-IV criterion “B” mania symptoms. However, in our current sample, all BD participants had type I BD by virtue of having had at least one full-duration manic episode. Children presenting with irritable mood only (i.e., without elated or expansive mood) were not included. Therefore, the BD group meet Leibenluft's “narrow phenotype” pediatric BD criteria, an advantage ensuring that all met a rigorous definition of BD. Youth with BD were not excluded for comorbid behavioral disorders (e.g., ODD, ADHD, etc.).

TDC ($N = 26$) inclusion criteria were (1) no current or lifetime psychiatric illness or substance abuse/dependence in the child participant and (2) no history of psychiatric illness in any first-degree relatives, as indicated by inquiry of one of the parents.

As is common in neuroimaging studies of children with BD, BD participants were allowed to remain on their outpatient medication regimens since this was not a treatment study. Participants taking stimulant medications were asked, but not required, to hold these medications for 4 drug half-lives before behavioral testing, which is a common practice in clinical care (e.g., weekends, holidays, etc.).

2.2. Neuropsychiatric measures

Overall functional impairment in the BD participants was assessed using clinician ratings on the Children's Global Assessment Scale (CGAS) (Shaffer et al., 1983). For the BD group, current symptoms (e.g., week of testing) of mania and depression were assessed using the Young Mania Rating Scale (YMRS) and Children's Depression Rating Scale (CDRS) respectively (Young et al., 1978; Poznanski and Mokros, 1996).

The Children's Behavior Checklist (CBCL) was also completed by parents to assess various internalizing and externalizing difficulties (Achenbach et al., 1991).

2.3. Neuroimaging acquisition procedures

MR imaging was conducted on a Siemens Tim Trio 3 T scanner with a 12-channel head coil with an imaging protocol that included a T_1-weighted MPRAGE acquisition and a diffusion-weighted GRAPPA acquisition. The T_1-weighted acquisition had repetition time 2250 ms, echo time 2.98 ms, T_1 time 900 ms, flip angle 9°, 160 slices, field-of-view 256 mm, $1 \times 1 \times 1$ mm^3 voxels, and total duration 7.36 min. The diffusion-weighted acquisition had repetition time 10,060 ms, echo time 103 ms, 70 slices, 64 directions, b-value 1000 s/mm^2, $1.8 \times 1.8 \times 1.8$ mm^3 voxels, one baseline scan without diffusion weighting, and total duration 12.56 min.

2.4. Neuroimaging analysis procedures

2.4.1. Diffusion-weighted MRI preprocessing

The dMRIs were processed to measure regional averages of diffusion tensor parameters and to reconstruct fiber bundle with multi-fiber modeling to improve accuracy in crossing fiber regions. The dMRIs were corrected for motion and eddy current artifacts by affine registration of each dMRI to the baseline scan (i.e. b = 0 s/mm^2) using the FSL 5.0 (Jenkinson et al., 2012). The orientations of the gradient vectors were also corrected by the rotation induced by these registrations (Leemans and Jones, 2009). Denoising was performed using the DWI-JointRicianLMMSEFilter module in 3D Slicer 4.4 (Tristán-Vega and Aja-Fernández, 2010). A mask of brain tissue was extracted from the baseline scan using FSL BET (Smith, 2002). Two types of diffusion models were used in the analysis. To characterize microstructural changes, diffusion tensor models were estimated using FSL DTIFIT, and the following tensor metrics were computed: FA, MD, axial diffusivity (AD), radial diffusivity (RD) (Basser and Pierpaoli, 1996; Le Bihan et al., 2001). Multiple diffusion parameters were included in the analysis because they provide sensitivity to complementary aspects of tissue microstructure (Beaulieu, 2002; Tournier et al., 2011) including axonal organization, density, and myelination (Wozniak and Lim, 2006). To characterize brain connectivity with tractography, multi-compartment ball-and-sticks diffusion models were estimated using FSL XFIBRES (Behrens et al., 2007), including two fiber compartments per voxel. Next, we describe steps taken to make quantitative measurements of brain structure that are comparable across the population (Fig. 1), including region-based analysis of cortical thickness and white matter microstructure and tractography-based analysis of white matter connectivity.

2.4.2. Region-based analysis

Regional averages of cortical thickness were computed using the high-resolution T_1-weighted MRI of each subject and regional averages of tensor parameters were computed by multimodal analysis with the dMRI data. Each T_1-weighted volume was processed using Freesurfer 5.0 (Fischl, 2012) to estimate cortical thickness (Fischl and Dale, 2000), to parcellate gray and white matter with the Desikan-Killiany (DK) atlas (Desikan et al., 2006), to segment of the corpus callosum (CC), and to estimate intra-cranial volume (ICV). The regional average of cortical thickness within each DK gray matter area was computed and retained for statistical analysis. Tensor parameters were measured in superficial white matter of each DK region and the subdivisions of the CC using the following steps. The T_1-weighted MRI was registered to the diffusion-weighted MRI using FSL FLIRT with an affine transformation using mutual information between T_1-weighted scan and the baseline scan from the diffusion-weighted MRI. To avoid resampling of the high-resolution regions of interest (ROIs), each diffusion tensor image was transformed to subject T_1-space. The region average of each diffusion tensor parameter was computed within each DK and CC white matter area and retained for statistical analysis (Cabeen et al., 2017).

2.4.3. Study template construction

For the tractography-based analysis, a study-specific diffusion tensor template was constructed using DTI-TK 2.3.1 (Zhang et al., 2007). The template was created by iteratively deforming and averaging the population imaging data using the tensor-based deformable registration algorithm in DTI-TK with finite strain tensor reorientation and the deviatoric tensor similarity metric. The template was used to define ROIs for delineating tracts-of-interest (TOIs) as follows. For each TOI, two inclusion ROIs and one exclusion ROI were drawn in template space using ITK-SNAP (Yushkevich et al., 2006). The inclusion masks were placed at opposite ends of each tractography bundle, and they were drawn in reference to standard white matter atlases (Catani and de Schotten, 2012; Wakana et al., 2007). The exclusion masks were drawn to exclude erroneous fibers that stray outside the expected bundle trajectory. The TOIs included: left and right anterior thalamic radiation (ATR), left and right cingulum (CING), left and right cortico-spinal tract (CST), left and right uncinate (UNC), left and right inferior longitudinal fasciculus (ILF), left and right inferior fronto-occipital fasciculus (IFOF), left and right fornix (FORN), and five sections of the corpus callosum selected using the Freesurfer CC labels (Fig. 1).

2.4.4. Tractography-based analysis

Tractography was used to characterize brain connectivity of each TOI. Whole brain tractography was performed using an extension of the standard streamline approach (Zhang et al., 2003) to use multiple fibers per voxels (Cabeen et al., 2016). The following parameters were used: four seeds per voxel, an angle threshold of 45 degrees, a minimum length of 10 mm, and a minimum volume fraction of 0.075. During tracking, a kernel regression estimation framework (Cabeen et al., 2016) was used for smooth interpolation of the multi-fiber ball-and-sticks models with a Gaussian kernel with a spatial bandwidth of 1.5 mm and voxel neighborhood of $5 \times 5 \times 5$. The masks for each TOI were deformed from the study template to subject space and then used to delineate each bundle from the whole brain fibers. For both whole brain fibers and TOIs, the following bundle metrics were computed: bundle volume, average track length, and bundle-average diffusion tensor parameters (Correia et al., 2008).

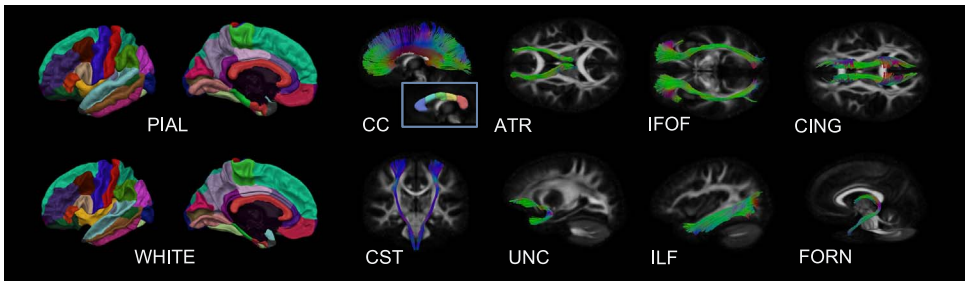

Fig. 1. Regions-of-interest and fiber bundles examined in the analysis. Surface renderings of the gray and white matter regions are shown in the left two columns. Streamtube tractography renderings of the in the study-specific atlas are shown in the other columns. The corpus callosum shows both the fibers as well as the five subdivisions used in the analysis.

2.5. Statistical analysis

The imaging metrics were statistically analyzed using regression models to assess group differences between TDC and BD youths and how they relate to age. Our analytic approach was guided by a desire to balance between an a priori focus on the fronto-temporal-striatal circuit implicated in BD, while also being mindful not to over-constrain these analyses. Thus, we also used a whole-brain approach for exploratory analyses. Multiple linear regression models were estimated to relate each imaging metric to group, age, intracranial volume, and IQ. Intracranial volume was included as a covariate to account for differences in brain size, which could potentially influence bundle metrics through partial volume effects. IQ was also included as a covariate to avoid potential confounding effects due to anatomical variation related to intelligence. To test for differences in maturation rate, each model included an interaction between the age and group variables, that is, an age coefficient was included for each of the TDC and BD groups in the model and a *t*-test was performed. The analysis specifically tested for age effects in the BD group relative to the TDC group that reflect reduced structural integrity, based on previous MR imaging findings (Beaulieu, 2002; Toteja et al., 2015). So, cortical thickness, FA, AD, bundle volume and length were tested for decreases in the BD group, while RD and MD were tested for increases in the BD group. To account for multiple comparisons, False Discovery Rate (FDR) control was used with the Benjamini-Hochberg procedure (Benjamini and Hochberg, 1995). Effects were determined to be significant with a FDR *q*-value threshold of 0.05. The results were plotted using ggplot2 (Wickham, 2009), and 3D visualizations of the *q*-values and tractography were created using the Quantitative Imaging Toolkit (http://cabeen.io/qitwiki). All coefficients are reported in standardized units by fitting regressions to z-scores of age and the imaging metrics.

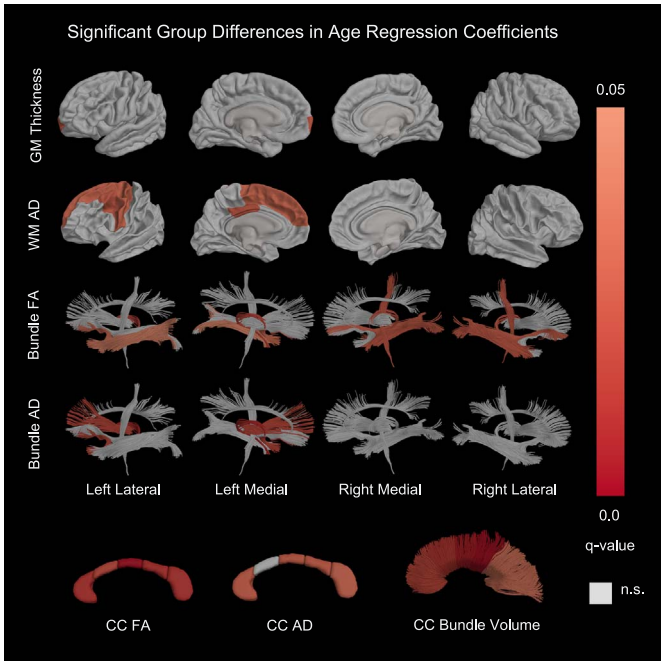

Fig. 2. Visualizations showing results from the statistical analysis. 3D renderings of anatomical models are shown with coloring to indicate significant differences (FDR *q*-value less than or equal to 0.05) in age effects between typically developing controls and bipolar disorder. The first row shows effects in cortical thickness in gray matter, and the second row shows effects in axial diffusivity measured in superficial white matter. The third and fourth rows show effects in fiber bundle fractional anisotropy and axial diffusivity, respectively. The fifth row shows effects in the corpus callosum, including fractional anisotropy, axial diffusivity, and fiber bundle volume. Non-significant (n.s.) bundle metrics were colored gray or not included in the visualization.

3. Results

3.1. Participants

With respect to demographics at MRI scan (Table 1), BD and TDC participants did not differ in age (Mean age BD = 13.9 + 2.6 years, TDC = 13.9 + 3.0 years; t(50) = −0.03, p = 1) or sex (BD male 18/26, female 8/26, TDC male 17/26, female 9/26; $X^2 = 0.09$, p = 1). The groups also had matched minimum age (8 years), median age (13.5 years), and maximum age (17 years). While both groups' mean WASI full-scale intelligence quotient (FSIQ) was in the "average" range, there was a statistically significant between-group difference (mean FSIQ BD = 104.6 + 10.8, TDC = 114.2 + 12.4; t(50) = −3.0, p = 0.005).

With respect to mood state and functional impairment of the BD group at the MRI scan, as a group, the BD participants were overall euthymic by clinician-administered mood ratings (mean YMRS = 7.3 ± 5.1, mean CDRS = 30.2 ± 12.8) and some impairment (mean CGAS = 63.8 + 15.4). Specifically, within the BD group, 69% (18/26) were euthymic (YMRS < 12, CDRS < 40), 11.5% (3/26) were depressed (YMRS < 12, CDRS ≥ 40), 8% (2/26) were hypomanic (YMRS = 13–24, CDRS < 40) and 11.5% (3/26) were mixed (YMRS > 12, CDRS ≥ 40). No participants were actively manic at the time of assessment (YMRS > 25, CDRS < 40).

Table 1
Sample Demographics. Note: *N* = 3 of 5 BD youths held their ADHD stimulants for at least four drug half-lives prior to their MRI scan.

	BD (N = 26)	TDC (N = 26)	
Demographics:			
Age:	13.9 ± 2.6 years	13.9 ± 3.0 years	$t(50) = -0.03$, $p = 1$
Sex:	8 female, 18 male	9 female, 17 male	$\chi 2 = 0.09$, $p = 1$
Full-Scale IQ:	104.6 ± 10.8	114.2 ± 12.4	$t(50) = -3.0$, $p = 0.005$
Young Mania Rating Scale (YMRS):	7.3 ± 5.1		
Children's Depression Rating Scale (CDRS):	30.2 ± 12.8		
Children's Global Assessment Scale (CGAS):	63.8 ± 15.4		
Comorbid Curred Psychiatric Diagnoses by Kiddie Schedule for Affective Disorders and Schizophrenia (K-SADS)[a]*:*			
ADHD:	N = 14 (54%)		
Oppositional Defiant Disorder (ODD):	N = 19 (73%)		
Generalized Anxiety Disorder (GAD):	N = 3 (11.5%)		
Social Phobia:	N = 2 (7.7%)		
Medications at scan:			
Lithium:	N = 8 (31%)		
Second generation anti-psychotic:	N = 15 (60%)		
Anti-epileptic drug:	N = 4 (15%)		
Serotenergic anti-depressant:	N = 5 (19%)		
ADHD stimulant:	N = 5 (19%)		

[a] KSADS "current" refers to past 6 months.

Table 2
Statistical results from the analysis. The first four numerical columns show the age regression coefficients of the control and bipolar disorder groups. The last four columns show results testing for differences in age coefficients between groups. Results were corrected for multiple comparisons using FDR, and the results listed here had an FDR q-value less than or equal to 0.05.

		TDC		BD		Difference			
Measure	**Structure**	**Beta**	**Stde**	**Beta**	**Stde**	**Beta**	**Stde**	**t-val**	**p-val**
Cortical Gray Matter:									
Thickness	Left Frontal Pole	−0.12	0.15	−0.86	0.16	−0.74	0.22	−3.3	0.0009
Cortical White Matter:									
AD	Left Caudal Middle Frontal	−0.01	0.18	−0.77	0.19	−0.75	0.26	−2.9	0.0025
AD	Left Posterior Cingulate	0.17	0.14	−0.45	0.15	−0.62	0.2	−3	0.0019
AD	Left Precentral	−0.06	0.17	−0.72	0.18	−0.66	0.25	−2.7	0.0053
AD	Left Superior Frontal	−0.04	0.18	−0.72	0.19	−0.68	0.26	−2.7	0.0052
AD	Left Temporal Pole	0	0.16	−0.67	0.17	−0.67	0.23	−2.9	0.0027
Corpus Callosum Regions:									
FA	CC Anterior Slice	0.29	0.19	−0.41	0.2	−0.7	0.27	−2.6	0.0066
FA	CC Middle Anterior Slice	0.29	0.21	−0.34	0.22	−0.63	0.3	−2.1	0.0204
FA	CC Central Slice	0.55	0.21	−0.52	0.22	−1.07	0.31	−3.5	0.0005
FA	CC Middle Posterior Slice	0.49	0.22	−0.3	0.23	−0.79	0.31	−2.5	0.0075
FA	CC Posterior Slice	0.41	0.15	−0.12	0.16	−0.53	0.22	−2.4	0.0092
AD	CC Anterior Slice	0.37	0.15	−0.14	0.16	−0.51	0.22	−2.3	0.0117
AD	CC Central Slice	0.42	0.2	−0.2	0.21	−0.62	0.29	−2.2	0.0176
AD	CC_Mid_Posterior	0.31	0.18	−0.32	0.19	−0.63	0.26	−2.4	0.0096
AD	CC Posterior Slice	0.08	0.04	−0.03	0.04	−0.11	0.05	−2	0.0255
RD	CC Central Slice	−0.26	0.17	0.43	0.18	0.69	0.25	2.8	0.0041
Fiber Bundles:									
Volume	CC Anterior Bundle	0.36	0.18	−0.23	0.19	−0.59	0.26	−2.3	0.0133
Volume	CC Middle Anterior Bundle	0.45	0.19	−0.25	0.2	−0.7	0.27	−2.5	0.007
Volume	CC Middle Bundle	0.74	0.18	−0.05	0.19	−0.79	0.26	−3	0.002
Volume	CC Middle Posterior Bundle	0.54	0.19	−0.41	0.2	−0.95	0.27	−3.5	0.0005
Volume	CC Posterior Bundle	0.2	0.19	−0.33	0.2	−0.53	0.28	−1.9	0.0331
Volume	Whole WM	0.36	0.17	−0.25	0.18	−0.61	0.25	−2.5	0.0087
FA	Left FORN	0.5	0.2	−0.35	0.21	−0.85	0.3	−2.9	0.0029
FA	Left ILF	0.4	0.2	−0.21	0.21	−0.61	0.29	−2.1	0.0204
FA	Left UNC	0.26	0.17	−0.34	0.18	−0.6	0.25	−2.4	0.0106
FA	Right CST	0.55	0.2	−0.17	0.21	−0.72	0.28	−2.5	0.0072
FA	Right FORN	0.51	0.21	−0.21	0.23	−0.72	0.31	−2.3	0.0122
FA	Right IFOF	0.26	0.18	−0.3	0.19	−0.57	0.26	−2.2	0.0176
FA	Right ILF	0.35	0.19	−0.34	0.2	−0.69	0.28	−2.5	0.0085
FA	Whole WM	0.54	0.18	0.04	0.19	−0.49	0.26	−1.9	0.0315
AD	Left ATR	0.07	0.13	−0.39	0.14	−0.46	0.19	−2.4	0.009
AD	Left FORN	0.28	0.14	−0.35	0.15	−0.63	0.2	−3.1	0.0014
AD	Left UNC	−0.04	0.14	−0.54	0.14	−0.5	0.2	−2.5	0.0078

3.2. Region-based analysis of cortical thickness

Of the 68 tested DK regions, only the left frontal pole showed significant group differences in age effects (Fig. 2, Table 2). Among TDC youths, the change with age was effectively zero, while BD youths had an age coefficient of −0.86, showing significantly greater thinning with age.

3.3. Region-based analysis of superficial white matter

Of the 68 tested DK white matter areas, five showed significant group differences in age effects in AD (Fig. 2, Table 2). Further examination showed that BD youths showed significant decreases in AD with age (Δ from −0.45 to −0.77), while TDC youths did not have significant changes in AD with age. The effects were found in the left hemisphere, and included superior frontal, caudal middle frontal, precentral, posterior cingulate, and temporal pole white matter. The largest effect size was found in left caudal middle frontal.

All regions of the corpus callosum showed significant group differences in age effects in FA, and some showed differences in RD and AD (Table 2). Additional analysis of these results showed that among TDC youths, FA was found to increase with age, AD was found to increase with age, and RD was found to decrease with age. Among BD youths, FA showed an opposite pattern of decreasing with age (Δ from −0.12 to −0.52), AD showed an opposite pattern of either negative or effectively zero slope (Δ from −0.029 to −0.32), and RD showed an opposite pattern of increasing with age (Δ = 0.43), The largest effect sizes were observed in the central CC.

3.4. Tractography-based analysis of fiber bundles

Of the bundles tested, nine showed significant group differences in age effects in one measure or another (Fig. 2, Table 2). Effects were found in bundle FA, AD, and volume; however, bundle length did not have a significant effect. Among TDC youths, FA significantly increased with age, AD was effectively stable across age, and volume increased with age in the CC. Among BD youths, all measures showed an opposite effect, with FA decreasing with age (Δ from −0.60 to −0.85), with AD decreasing with age (Δ from −0.46 to −0.63), and volume decreasing with age in the CC (Δ from −0.53 to −0.95). The largest effect sizes were observed in the corpus callosum and fornix. Among whole brain measures, TDC youths had increasing FA with age, while BD youths showed negligible changes with age (Δ = −0.49).

3.5. Post-hoc tests related to IQ

Because IQ was found to be slightly different between groups, all results included IQ as a covariate. We also performed post-hoc tests to examine the direct relationship between imaging metrics and IQ. We computed Pearson's correlation coefficient between IQ and each imaging metric that had a significant group effect, and tested whether the coefficient was significantly different from zero. None of these imaging

metrics were found to be significantly correlated to IQ, with or without FDR correction.

3.6. Post-hoc tests related to medication

Previous studies have observed changes in gray matter with medication (Sassi et al., 2002; Lyoo et al., 2010), so we conducted post-hoc tests to assess the possibility that medication load is associated with the effects observed in the present study. We summarized the medication load of each BPD participant with a numeric score of 0, 1, or 2 according to the procedures described by Phillips et al. (Phillips et al., 2008). This included medication load indices for anti-manic, anti-depressant, ADHD, and benzodiazepine medications, as well as an index of total medication load. We examined the hypothesis that the observed effects in age are in fact a reflection of variation in medication across age, and we accordingly tested the correlation between age and each medication load index. The tests revealed no significant relationship between medication load and age.

3.7. Supplementary material

The Supplemental material includes three tables summarizing the imaging parameters for each region and bundle of interest, including cortical thickness, tensor parameters, and tractography metrics.

4. Discussion

Our study provides a broad view of what multi-modal structural MR imaging can tell us regarding maturation rates of fronto-temporal-striatal neurocircuitry in pediatric BD. Our findings generally indicate that TDC and BD youths exhibit different maturation trajectories, as characterized by imaging metrics of cortical thickness, superficial white matter, and fiber bundle mapping of deep white matter. We will focus our discussion on the interpretation of findings related to our primary hypotheses regarding fronto-temporal-striatal areas; however, because the analysis included an exploratory component, we also discuss results from other brain areas, which are included in the tables and figures.

Our first main finding was that BD participants had relatively greater cortical thinning with age than TDC youths. Our finding of specific group differences in the left frontal pole aligns with prior studies demonstrating left PFC gray matter volume and density effects in BD (Dickstein, 2005; James et al., 2011). In the context of neural models of BD, our finding of decreased PFC gray matter maturation among BD youth may contribute to others who have found disturbances in emotional processing and executive control reflected in both the symptoms of BD as also in brain and behavioral deficits in related tasks (Wiggins et al., 2015; Wegbreit et al., 2016).

Our second main finding was that BD participants exhibited disrupted maturation trajectories in diffusion tensor imaging metrics of both superficial and deep white matter. These findings support previous work that has shown BD participants to have decreased tensor FA (Frazier et al., 2007; Gao et al., 2013; Gönenç et al., 2010; Adler et al., 2004; Kafantaris et al., 2009; Barnea-Goraly et al., 2010); however, our results showed strong effects in tensor AD as well. Effects in tensor AD were lateralized, specifically, in fiber bundles and superficial white matter regions that form the basis of left hemisphere fronto-temporal-striatal connectivity. Based on previous studies and the absence of effects in RD, the results may reflect group differences in axonal integrity in these regions (Song et al., 2002; Budde et al., 2009). Unlike AD, effects in tensor FA were present bilaterally in fiber bundles related to fronto-temporal-striatal connectivity, with more effects found in the temporal lobe than with AD. Since tensor parameters are coupled to some extent, the regions that showed only effects in FA may reflect more variation in fiber organization than they do myelination (Beaulieu, 2002; Wozniak and Lim, 2006). Together, these disruptions to fronto-temporal-striatal pathways likely reflect a variety of features of BD psychopathology, as these connections are crucial for coordinating the communications necessary for complex emotional behaviors, including response to emotional faces, response inhibition, and cognitive flexibility and adaptation to changing rewards and punishments (Wu et al., 2017; Wegbreit et al., 2015; Seymour et al., 2015; Brotman et al., 2007; Singh et al., 2010a, 2010b; Passarotti et al., 2010; Dickstein et al., 2016).

We also found strong effects throughout the corpus callosum, including bundle volume as well as tensor FA and tensor AD. Several other dMRI studies have shown that BD youth have disruptions in the integrity of the anterior corpus callosum compared to TDC youths (James et al., 2011; Barnea-Goraly et al., 2009; Saxena et al., 2012; Lagopoulos et al., 2013). Because these previous findings were primarily focused on TBSS metrics, the present study helps to broaden our picture of these effects through the combination of ROI analysis and tractography metrics. The corpus callosum plays a pivotal role in facilitating inter-hemispheric communication and has been linked to behaviors that may be found in mania, including aggression (Schutter and Harmon-Jones, 2013). However, it remains unclear if pediatric BD involves a developmental lag in corpus callosum maturation that eventually catches up in adulthood or if these represent neural alterations inherent in BD, whether the patient is a child or an adult. While only distally related, a recent article examining 22 dMRI studies found that anti-social behavior, including aggression, violence, and theft was related to white matter disruptions in the corpus callosum among adult, but not child, studies (Waller et al., 2017). Thus, the answer to the question about developmentally salient periods in corpus callosum development in BD could inform neuroimage-assisted diagnostic approaches, or the development of novel treatments, including cognitive remediation approaches.

Our study has several potential limitations, including sample size, cross-sectional design, participant age, imaging, and BD participants' ongoing treatment. Our study uses a relatively small sample of participants studied cross-sectionally. Future studies are required to confirm our findings in larger samples imaged repeatedly over time to have a truer sense of how these alterations change as children develop. Regarding participant age, our present study evaluated BD and TDC youth from ages 8–17 years old. Thus, while our data shows that BD youths diverge from TDC youths in their trajectory of cortical thickness and tensor metrics across development, further research along the lines of Toteja et al. are needed, whereby participants with and without BD across the lifespan are imaged using the same scanner and sequences are required to determine the course of this divergence from adolescence into adulthood. While there was a significant between-group difference in IQ, like previous studies (Shaw et al., 2006), both groups were within typical ranges. Nevertheless, future work could probe the relationship between IQ and the MRI measures in a large sample, and furthermore, relate these to deficits in executive function previously observed in BD (Wegbreit et al., 2016). The diffusion MR imaging sequence was another limitation of the study, and future studies could improve the diffusion acquisition by including multiple baselines, as this would enable the subsequent modeling to account for coil sensitivities, subject motion, geometric distortions due to susceptibility and eddy currents, and spatial variation in noise that may impact the modeling of subcortical structures and fiber bundles. Furthermore, while Freesurfer was used in the present study to analyze T1-weighted MR imaging data, other methods for subcortical segmentation, such as FSL FIRST and manual delineation, may offer improved performance in some cases as well (Morey et al., 2009). Another limitation was that BD youth were taking psychotropic medication when scanned. However, it would be unethical to stop their medications for a non-treatment neuroimaging study. Moreover, as it was a cross-sectional study, we do not have detailed prospective records about all medications previously used by each patient. Thus, it is possible that the observed between-group differences in cortical thickness and white matter may be impacted by these prior or ongoing treatments. Moreover, this is an important

question germane to all psychiatric disorders, and not just BD, though its answer is complicated by the reality in human imaging studies that it would be unethical not to treat those suffering from any psychiatric illness for several years for the sake of imaging or other research study. Ultimately, this may require translational studies using animal models whereby such issues would not come into play. However, this too will be complicated for BD where there are no well-validated animal models of mania. Expanding the scope of human imaging studies may also help elucidate the effect of medication; however, because treatment regimens are often diverse across patients, substantial sample sizes may be required to obtain the statistical power necessary to detect changes in white matter maturation due to medication. Nevertheless, our study integrating novel cross-modality structural MRI and dMRI methods provides an important new lead on the neurodevelopmental circuit mechanisms of BD.

In considering what is ahead based our findings, the ultimate question from our study is how can it improve our ability to understand the neurobiology of BD and to treat children and adolescents suffering from BD? While no neuroimaging parameter has been shown to be a replicated sensitive and specific biomarker for BD in any age group, the present study demonstrates the strength of advanced computational image analysis in understanding the anatomical variation exhibited in BD. This study includes some specific advancements relative to previous tractography-based studies of BD. We used multi-fiber tractography framework to improve anatomical accuracy of fiber bundle reconstruction, and furthermore, used a study-specific template and deformable tensor-based registration algorithm, which have both been shown to improve registration quality and improve sensitivity in dMRI studies (Zhang et al., 2007; Van Hecke et al., 2011). Going forward, advances in these computational approaches will likely be increasingly important in understanding the anatomical basis of BD psychopathology. In particular, there is much to gain by improving dMRI acquisitions and modeling approaches. While the tensor model is highly sensitive to changes in microstructure, it can potentially conflate distinct microstructural properties (Wheeler-Kingshott and Cercignani, 2009; Jones et al., 2013). With more advanced data acquisitions and models, some of the more subtle effects can be disentangled with more anatomically specific microstructure metrics (Fieremans et al., 2011; Zhang et al., 2012). Novel applications of these approaches could include longitudinal imaging studies to compare the neurodevelopmental trajectories of BD and TDC youths, and also potential effects of treatment as well as non-adherence, thus allowing neuroimaging to address important fundamental and clinically-relevant issues in pediatric BD (Pompili et al., 2013). Nevertheless, our preliminary findings show that multimodal structural MR imaging metrics provide a potentially useful tool for understanding the trajectory taken during neurodevelopment.

5. Conclusions

Our study provides further evidence of widespread fronto-temporal-striatal alterations in BD; however, our findings specifically shed more light on how developmental trajectories also differ between TDC and BD youths. Using a multimodal imaging approach, we found group differences in gray matter cortical thickness of the left frontal pole, and in white matter pathways that form fronto-temporal-striatal circuitry, and widespread effects in the corpus callosum. Beyond these specific findings, we also showed how computational image analysis can provide a broader understanding of developmental trajectories in BD by integrating multiple modalities. Because of the preliminary nature of the present study, further studies are warranted to investigate these effects in larger populations, particularly to examine the brain areas identified in this study for longitudinal changes and changes in response to treatment.

Acknowledgements

This work was supported by funding from the National Institute of Mental Health (NIMH, K22MH074945, PI = D Dickstein) and the Brown Institute for Brain Science Graduate Research Award. We also truly appreciate the child participants' and their parents' help, without which this study would not be possible.

Contributors

DP Dickstein was responsible for study design, data collection, and manuscript preparation, DH Laidlaw was responsible for data analysis design and manuscript preparation, and RP Cabeen was responsible for design and implementation of the data analysis, data visualization, and manuscript preparation.

Conflict of interest

On behalf of all authors, the corresponding author states that there is no conflict of interest.

Appendix A. Supporting information

Supplementary data associated with this article can be found in the online version at http://dx.doi.org/10.1016/j.pscychresns.2017.12.006.

References

Achenbach, T.M., Howell, C.T., Quay, H.C., Conners, C.K., Bates, J.E., 1991. National survey of problems and competencies among four-to sixteen-year-olds: parents' reports for normative and clinical samples. Monogr. Soc. Res. Child Dev. 130.

Adleman, N.E., Kayser, R., Dickstein, D., Blair, R.J.R., Pine, D., Leibenluft, E., 2011. Neural correlates of reversal learning in severe mood dysregulation and pediatric bipolar disorder. J. Am. Acad. Child Adolesc. Psychiatry 50 (11), 1173–1185.

Adler, C.M., Holland, S.K., Schmithorst, V., Wilke, M., Weiss, K.L., Pan, H., et al., 2004. Abnormal frontal white matter tracts in bipolar disorder: a diffusion tensor imaging study. Bipolar Disord. 6 (3), 197–203.

Adler, C.M., Adams, J., DelBello, M.P., Holland, S.K., Schmithorst, V., Levine, A., et al., 2006. Evidence of white matter pathology in bipolar disorder adolescents experiencing their first episode of mania: a diffusion tensor imaging study. Am. J. Psychiatry 163 (2), 322–324.

Baldessarini, R.J., Bolzani, L., Cruz, N., Jones, P.B., Lai, M., Lepri, B., et al., 2010. Onset-age of bipolar disorders at six international sites. J. Affect. Disord. 121 (1), 143–146.

Baldessarini, R.J., Tondo, L., Vázquez, G.H., Undurraga, J., Bolzani, L., Yildiz, A., et al., 2012. Age at onset versus family history and clinical outcomes in 1,665 international bipolar-I disorder patients. World Psychiatry 11 (1), 40–46.

Barnea-Goraly, N., Chang, K.D., Karchemskiy, A., Howe, M.E., Reiss, A.L., 2009. Limbic and corpus callosum aberrations in adolescents with bipolar disorder: a tract-based spatial statistics analysis. Biol. Psychiatry 66 (3), 238–244.

Barnea-Goraly, N., Lotspeich, L.J., Reiss, A.L., 2010. Similar white matter aberrations in children with autism and their unaffected siblings: a diffusion tensor imaging study using tract-based spatial statistics. Arch. Gen. Psychiatry 67, 1052–1060.

Basser, P.J., Pierpaoli, C., 1996. Microstructural and physiological features of tissues elucidated by quantitative-diffusion-tensor MRI. Journal of magnetic resonance. Series B 111 (3), 209.

Beaulieu, C., 2002. The basis of anisotropic water diffusion in the nervous system–a technical review. NMR Biomed. 15 (7–8), 435–455.

Behrens, T.E.J., Berg, H.J., Jbabdi, S., Rushworth, M.F.S., Woolrich, M.W., 2007. Probabilistic diffusion tractography with multiple fibre orientations: what can we gain? Neuroimage 34 (1), 144–155.

Benjamini, Y., Hochberg, Y., 1995. Controlling the false discovery rate: a practical and powerful approach to multiple testing. J. R. Stat. Soc. Ser. B (Methodol.) 289–300.

Blader, J.C., Carlson, G.A., 2007. Increased rates of bipolar disorder diagnoses among US child, adolescent, and adult inpatients, 1996–2004. Biol. Psychiatry 62 (2), 107–114.

Blumberg, H.P., Kaufman, J., Martin, A., Whiteman, R., Zhang, J.H., Gore, J.C., et al., 2003. Amygdala and hippocampal volumes in adolescents and adults with bipolar disorder. Arch. Gen. Psychiatry 60 (12), 1201–1208.

Brotman, M.A., Kassem, L., Reising, M.M., Guyer, A.E., Dickstein, D.P., Rich, B.A., et al., 2007. Parental diagnoses in youth with narrow phenotype bipolar disorder or severe mood dysregulation. Am. J. Psychiatry 164 (8), 1238–1241.

Brotman, M.A., Rich, B.A., Guyer, A.E., Lunsford, J.R., Horsey, S.E., Reising, M.M., et al., 2009. Amygdala activation during emotion processing of neutral faces in children with severe mood dysregulation versus ADHD or bipolar disorder. Am. J. Psychiatry 167 (1), 61–69.

Budde, M.D., Xie, M., Cross, A.H., Song, S.K., 2009. Axial diffusivity is the primary correlate of axonal injury in the experimental autoimmune encephalomyelitis spinal

cord: a quantitative pixelwise analysis. J. Neurosci. 29 (9), 2805–2813.
Cabeen, R.P., Bastin, M.E., Laidlaw, D.H., 2016. Kernel regression estimation of fiber orientation mixtures in diffusion MRI. NeuroImage 127, 158–172.
Cabeen, R.P., Bastin, M.E., Laidlaw, D.H., 2017. A Comparative evaluation of voxel-based spatial mapping in diffusion tensor imaging. NeuroImage 146, 100–112.
Catani, M., de Schotten, M.T., 2012. Atlas of Human Brain Connections. Oxford University Press.
Wheeler-Kingshott, C.A., Cercignani, M., 2009. About "axial" and "radial" diffusivities. Magn. Reson. Med. 61 (5), 1255–1260.
Chang, K., Karchemskiy, A., Barnea-Goraly, N., Garrett, A., Simeonova, D.I., Reiss, A., 2005. Reduced amygdalar gray matter volume in familial pediatric bipolar disorder. J. Am. Acad. Child Adolesc. Psychiatry 44 (6), 565–573.
Correia, S., Lee, S.Y., Voorn, T., Tate, D.F., Paul, R.H., Zhang, S., et al., 2008. Quantitative tractography metrics of white matter integrity in diffusion-tensor MRI. Neuroimage 42 (2), 568–581.
Desikan, R.S., Ségonne, F., Fischl, B., Quinn, B.T., Dickerson, B.C., Blacker, D., et al., 2006. An automated labeling system for subdividing the human cerebral cortex on MRI scans into gyral based regions of interest. Neuroimage 31 (3), 968–980.
Deveney, C.M., Connolly, M.E., Haring, C.T., Bones, B.L., Reynolds, R.C., Kim, P., et al., 2013. Neural mechanisms of frustration in chronically irritable children. Am. J. Psychiatry 170 (10), 1186–1194.
Dickstein, D.P., Milham, M.P., Nugent, A.C., Drevets, W.C., Charney, D.S., Pine, D.S., et al., 2005. Frontotemporal alterations in pediatric bipolar disorder: results of a voxel-based morphometry study. Arch. General. Psychiatry 62 (7), 734–741.
Dickstein, D.P., Rich, B.A., Roberson-Nay, R., Berghorst, L., Vinton, D., Pine, D.S., et al., 2007. Neural activation during encoding of emotional faces in pediatric bipolar disorder. Bipolar Disord. 9 (7), 679–692.
Dickstein, D.P., Axelson, D., Weissman, A.B., Yen, S., Hunt, J.I., Goldstein, B.I., et al., 2016. Cognitive flexibility and performance in children and adolescents with threshold and sub-threshold bipolar disorder. Eur. Child Adolesc. Psychiatry 25 (6), 625–638.
Dickstein, D.P., Finger, E.C., Skup, M., Pine, D.S., Blair, J.R., Leibenluft, E., 2010. Altered neural function in pediatric bipolar disorder during reversal learning. Bipolar Disord. 12 (7), 707–719.
DelBello, M.P., Zimmerman, M.E., Mills, N.P., Getz, G.E., Strakowski, S.M., 2004. Magnetic resonance imaging analysis of amygdala and other subcortical brain regions in adolescents with bipolar disorder. Bipolar Disord. 6 (1), 43–52.
Fieremans, E., Jensen, J.H., Helpern, J.A., 2011. White matter characterization with diffusional kurtosis imaging. Neuroimage 58 (1), 177–188.
Fischl, B., Dale, A.M., 2000. Measuring the thickness of the human cerebral cortex from magnetic resonance images. Proc. Natl. Acad. Sci. 97 (20), 11050–11055.
Fischl, B., 2012. FreeSurfer. Neuroimage 62.2, 774–781.
Frazier, J.A., Breeze, J.L., Papadimitriou, G., Kennedy, D.N., Hodge, S.M., Moore, C.M., et al., 2007. White matter abnormalities in children with and at risk for bipolar disorder. Bipolar Disord. 9 (8), 799–809.
Gao, W., Jiao, Q., Qi, R., Zhong, Y., Lu, D., Xiao, Q., et al., 2013. Combined analyses of gray matter voxel-based morphometry and white matter tract-based spatial statistics in pediatric bipolar mania. J. Affect. Disord. 150 (1), 70–76.
Gönenç, A., Frazier, J.A., Crowley, D.J., Moore, C.M., et al., 2010. Combined diffusion tensor imaging and transverse relaxometry in early-onset bipolar disorder. J. Am. Acad. Child Adolesc. Psychiatry 49 (12), 1260–1268.
Hajek, T., Kopecek, M., Kozeny, J., Gunde, E., Alda, M., Höschl, C., 2009. Amygdala volumes in mood disorders—meta-analysis of magnetic resonance volumetry studies. J. Affect. Disord. 115 (3), 395–410.
Ishida, T., Donishi, T., Iwatani, J., Yamada, S., Takahashi, S., Ukai, S., et al., 2017. Interhemispheric disconnectivity in the sensorimotor network in bipolar disorder revealed by functional connectivity and diffusion tensor imaging analysis. Heliyon 3 (6), e00335.
Holtmann, M., Duketis, E., Poustka, L., Zepf, F.D., Poustka, F., Bölte, S., 2010. Bipolar disorder in children and adolescents in Germany: national trends in the rates of in-patients, 2000–2007. Bipolar Disord. 12 (2), 155–163.
James, A., Hough, M., James, S., Burge, L., Winmill, L., Nijhawan, S., et al., 2011. Structural brain and neuropsychometric changes associated with pediatric bipolar disorder with psychosis. Bipolar Disord. 13, 16–27.
Jenkinson, M., Beckmann, C.F., Behrens, T.E., Woolrich, M.W., Smith, S.M., 2012. Fsl. Neuroimage 62 (2), 782–790.
Jones, D.K., Knösche, T.R., Turner, R., 2013. White matter integrity, fiber count, and other fallacies: the do's and don'ts of diffusion MRI. Neuroimage 73, 239–254.
Kafantaris, V., Kingsley, P., Ardekani, B., Saito, E., Lencz, T., Lim, K., Szeszko, P., 2009. Lower orbital frontal white matter integrity in adolescents with bipolar I disorder. J. Am. Acad. Child Adolesc. Psychiatry 48 (1), 79–86.
Kalmar, J.H., Wang, F., Chepenik, L.G., Womer, F.Y., Jones, M.M., Pittman, B., et al. 2009. Relation Between Amygdala Structure and Function in Adolescents with Bipolar Disorder.
Kim, P., Thomas, L.A., Rosen, B.H., Moscicki, A.M., Brotman, M.A., Zarate Jr, C.A., et al., 2012. Differing amygdala responses to facial expressions in children and adults with bipolar disorder. Am. J. Psychiatry 169 (6), 642–649.
Lagopoulos, J., Hermens, D.F., Hatton, S.N., Tobias-Webb, J., Griffiths, K., Naismith, S.L., et al., 2013. Microstructural white matter changes in the corpus callosum of young people with bipolar disorder: a diffusion tensor imaging study. PLoS One 8 (3), e59108.
Leboyer, M., Henry, C., Paillere-Martinot, M.L., Bellivier, F., 2005. Age at onset in bipolar affective disorders: a review. Bipolar Disord. 7 (2), 111–118.
Leemans, A., Jones, D.K., 2009. The B-matrix must be rotated when correcting for subject motion in DTI data. Magn. Reson. Med. 61 (6), 1336–1349.
Leibenluft, E., Rich, B.A., Vinton, D.T., Nelson, E.E., Fromm, S.J., Berghorst, L.H., et al., 2007a. Neural circuitry engaged during unsuccessful motor inhibition in pediatric bipolar disorder. Am. J. Psychiatry.
Leibenluft, E., Rich, B.A., Vinton, D.T., Nelson, E.E., Fromm, S.J., Berghorst, L.H., et al., 2007b. Neural circuitry engaged during unsuccessful motor inhibition in pediatric bipolar disorder. Am. J. Psychiatry.
Le Bihan, D., Mangin, J.F., Poupon, C., Clark, C.A., Pappata, S., Molko, N., Chabriat, H., 2001. Diffusion tensor imaging: concepts and applications. J. Magn. Reson. Imaging 13 (4), 534–546.
Lu, L.H., Zhou, X.J., Fitzgerald, J., Keedy, S.K., Reilly, J.L., Passarotti, A.M., et al., 2012. Microstructural abnormalities of white matter differentiate pediatric and adult-onset bipolar disorder. Bipolar Disord. 14 (6), 597–606.
Lyoo, I.K., Dager, S.R., Kim, J.E., Yoon, S.J., Friedman, S.D., Dunner, D.L., Renshaw, P.F., 2010. Lithium-induced gray matter volume increase as a neural correlate of treatment response in bipolar disorder: a longitudinal brain imaging study. Neuropsychopharmacology 35 (8), 1743–1750.
Moreno, C., Laje, G., Blanco, C., Jiang, H., Schmidt, A.B., Olfson, M., 2007. National trends in the outpatient diagnosis and treatment of bipolar disorder in youth. Arch. Gen. Psychiatry 64 (9), 1032–1039.
Morey, R.A., Petty, C.M., Xu, Y., Hayes, J.P., Wagner, H.R., Lewis, D.V., LaBar, K.S., Styner, M., McCarthy, G., 2009. A comparison of automated segmentation and manual tracing for quantifying hippocampal and amygdala volumes. Neuroimage 45 (3), 855–866.
Mwangi, B., Spiker, D., Zunta-Soares, G.B., Soares, J.C., 2014. Prediction of pediatric bipolar disorder using neuroanatomical signatures of the amygdala. Bipolar Disord. 16 (7), 713–721.
Passarotti, A.M., Sweeney, J.A., Pavuluri, M.N., 2010. Neural correlates of response inhibition in pediatric bipolar disorder and attention deficit hyperactivity disorder. Psychiatry Res.: Neuroimaging 181 (1), 36–43.
Pavuluri, M.N., O'Connor, M.M., Harral, E., Sweeney, J.A., 2007. Affective neural circuitry during facial emotion processing in pediatric bipolar disorder. Biol. Psychiatry 62 (2), 158–167.
Pavuluri, M.N., Yang, S., Kamineni, K., Passarotti, A.M., Srinivasan, G., Harral, E.M., et al., 2009. Diffusion tensor imaging study of white matter fiber tracts in pediatric bipolar disorder and attention-deficit/hyperactivity disorder. Biol. Psychiatry 65 (7), 586–593.
Pfeifer, J.C., Welge, J., Strakowski, S.M., Adler, C., Delbello, M.P., 2008. Meta-analysis of amygdala volumes in children and adolescents with bipolar disorder. J. Am. Acad. Child Adolesc. Psychiatry 47 (11), 1289–1298.
Phillips, M.L., Travis, M.J., Fagiolini, A., Kupfer, D.J., 2008. Medication effects in neuroimaging studies of bipolar disorder. Am. J. Psychiatry 165 (3), 313–320.
Pompili, M., Venturini, P., Palermo, M., Stefani, H., Seretti, M.E., Lamis, D.A., Serafini, G., Amore, M., Girardi, P., 2013. Mood disorders medications: predictors of non-adherence–review of the current literature. Expert Rev. Neurother. 13 (7), 809–825.
Poznanski, E.O., Mokros, H.B., 1996. Children's Depression Rating Scale, Revised (CDRS-R). Western Psychological Services, Los Angeles.
Rich, B.A., Fromm, S.J., Berghorst, L.H., Dickstein, D.P., Brotman, M.A., Pine, D.S., et al., 2008. Neural connectivity in children with bipolar disorder: impairment in the face emotion processing circuit. J. Child Psychol. Psychiatry 49 (1), 88–96.
Rich, B.A., Holroyd, T., Carver, F.W., Onelio, L.M., Mendoza, J.K., Cornwell, B.R., et al., 2010. A preliminary study of the neural mechanisms of frustration in pediatric bipolar disorder using magnetoencephalography. Depress. Anxiety 27 (3), 276–286.
Sassi, R.B., Nicoletti, M., Brambilla, P., Mallinger, A.G., Frank, E., Kupfer, D.J., Keshavan, M.S., Soares, J.C., 2002. Increased gray matter volume in lithium-treated bipolar disorder patients. Neurosci. Lett. 329 (2), 243–245.
Saxena, K., Tamm, L., Walley, A., Simmons, A., Rollins, N., Chia, J., et al., 2012. A preliminary investigation of corpus callosum and anterior commissure aberrations in aggressive youth with bipolar disorders. J. Child Adolesc. Psychopharmacol. 22 (2), 112–119.
Shaffer, D., Gould, M.S., Brasic, J., Ambrosini, P., Fisher, P., Bird, H., et al., 1983. A children's global assessment scale (CGAS). Arch. Gen. Psychiatry 40 (11), 1228–1231.
Shaw, P., Lerch, J., Greenstein, D., Sharp, W., Clasen, L., Evans, A., et al., 2006. Longitudinal mapping of cortical thickness and clinical outcome in children and adolescents with attention-deficit/hyperactivity disorder. Arch. Gen. Psychiatry 63 (5), 540–549.
Singh, M.K., Chang, K.D., Mazaika, P., Garrett, A., Adleman, N., Kelley, R., Howe, M., Reiss, A., 2010a. Neural correlates of response inhibition in pediatric bipolar disorder. J. Child Adolesc. Psychopharmacol. 20 (1), 15–24.
Schutter, D.J., Harmon-Jones, E., 2013. The corpus callosum: a commissural road to anger and aggression. Neurosci. Biobehav. Rev. 37 (10), 2481–2488.
Seymour, K.E., Kim, K.L., Cushman, G.K., Puzia, M.E., Weissman, A.B., Galvan, T., Dickstein, D.P., 2015. Affective processing bias in youth with primary bipolar disorder or primary attention-deficit/hyperactivity disorder. Eur. Child Adolesc. Psychiatry 24 (11), 1349–1359.
Singh, M.K., Chang, K.D., Mazaika, P., Garrett, A., Adleman, N., Kelley, R., et al., 2010b. Neural correlates of response inhibition in pediatric bipolar disorder. J. Child Adolesc. Psychopharmacol. 20 (1), 15–24.
Smith, S.M., 2002. Fast robust automated brain extraction. Hum. Brain Mapp. 17 (3), 143–155.
Song, S.K., Sun, S.W., Ramsbottom, M.J., Chang, C., Russell, J., Cross, A.H., 2002. Dysmyelination revealed through MRI as increased radial (but unchanged axial) diffusion of water. Neuroimage 17 (3), 1429–1436.
Stoddard, J., Hsu, D., Reynolds, R.C., Brotman, M.A., Ernst, M., Pine, D.S., et al., 2015. Aberrant amygdala intrinsic functional connectivity distinguishes youths with bipolar disorder from those with severe mood dysregulation. Psychiatry Res.: Neuroimaging 231 (2), 120–125.
Toteja, N., Guvenek-Cokol, P., Ikuta, T., Kafantaris, V., Peters, B.D., Burdick, K.E., et al.,

2015. Age-associated alterations in corpus callosum white matter integrity in bipolar disorder assessed using probabilistic tractography. Bipolar Disord. 17 (4), 381–391.
Tournier, J.D., Mori, S., Leemans, A., 2011. Diffusion tensor imaging and beyond. Magn. Reson. Med. 65 (6), 1532–1556.
Tristán-Vega, A., Aja-Fernández, S., 2010. DWI filtering using joint information for DTI and HARDI. Med. Image Anal. 14 (2), 205–218.
Van Hecke, W., Leemans, A., Sage, C.A., Emsell, L., Veraart, J., Sijbers, J., et al., 2011. The effect of template selection on diffusion tensor voxel-based analysis results. Neuroimage 55 (2), 566–573.
Wakana, S., Caprihan, A., Panzenboeck, M.M., Fallon, J.H., Perry, M., Gollub, R.L., et al., 2007. Reproducibility of quantitative tractography methods applied to cerebral white matter. Neuroimage 36 (3), 630–644.
Waller, R., Dotterer, H.L., Murray, L., Maxwell, A.M., Hyde, L.W., 2017. White-matter tract abnormalities and antisocial behavior: a systematic review of diffusion tensor imaging studies across development. NeuroImage: Clin.
Wegbreit, E., Weissman, A.B., Cushman, G.K., Puzia, M.E., Kim, K.L., Leibenluft, E., et al., 2015. Facial emotion recognition in childhood-onset bipolar I disorder: an evaluation of developmental differences between youths and adults. Bipolar Disord. 17 (5), 471–485.
Wegbreit, E., Cushman, G.K., Weissman, A.B., Bojanek, E., Kim, K.L., Leibenluft, E., et al., 2016. Reversal-learning deficits in childhood-onset bipolar disorder across the transition from childhood to young adulthood. J. Affect. Disord. 203, 46–54.
Wickham, H., 2009. ggplot2: Elegant Graphics for Data Analysis. Springer Science & Business Media.
Wiggins, J.L., Adleman, N.E., Kim, P., Oakes, A.H., Hsu, D., Reynolds, R.C., et al., 2015. Developmental differences in the neural mechanisms of facial emotion labeling. Social. Cogn. Affect. Neurosci. 11 (1), 172–181.
Wiggins, J.L., Brotman, M.A., Adleman, N.E., Kim, P., Wambach, C.G., Reynolds, R.C., et al., 2017. Neural markers in pediatric bipolar disorder and familial risk for bipolar disorder. J. Am. Acad. Child Adolesc. Psychiatry 56 (1), 67–78.
Wozniak, J.R., Lim, K.O., 2006. Advances in white matter imaging: a review of in vivo magnetic resonance methodologies and their applicability to the study of development and aging. Neurosci. Biobehav. Rev. 30 (6), 762–774.
Wu, M.J., Mwangi, B., Bauer, I.E., Passos, I.C., Sanches, M., Zunta-Soares, G.B., Meyer, T.D., Hasan, K.M., Soares, J.C., 2017. Identification and individualized prediction of clinical phenotypes in bipolar disorders using neurocognitive data, neuroimaging scans and machine learning. Neuroimage 145, 254–264.
Young, R.C., Biggs, J.T., Ziegler, V.E., Meyer, D.A., 1978. A rating scale for mania: reliability, validity and sensitivity. Br. J. Psychiatry 133 (5), 429–435.
Yushkevich, P.A., Piven, J., Hazlett, H.C., Smith, R.G., Ho, S., Gee, J.C., et al., 2006. User-guided 3D active contour segmentation of anatomical structures: significantly improved efficiency and reliability. Neuroimage 31 (3), 1116–1128.
Zhang, S., Demiralp, C., Laidlaw, D.H., 2003. Visualizing diffusion tensor MR images using streamtubes and streamsurfaces. Vis. Comput. Graph. IEEE Trans. 9 (4), 454–462.
Zhang, H., Avants, B.B., Yushkevich, P., Woo, J.H., Wang, S., McCluskey, L.F., et al., 2007. High-dimensional spatial normalization of diffusion tensor images improves the detection of white matter differences: an example study using amyotrophic lateral sclerosis. Med. Imaging IEEE Trans. 26 (11), 1585–1597.
Zhang, H., Schneider, T., Wheeler-Kingshott, C.A., Alexander, D.C., 2012. NODDI: practical in vivo neurite orientation dispersion and density imaging of the human brain. Neuroimage 61 (4), 1000–1016.